– Filtration

"The capture of aerosol particles by filtration is the most common method for aerosol sampling and is a widely used method for air cleaning. Filtration is a simple versatile, and economical means for collecting aerosol particles"

" There are different types of filters. From them, the common one is "fibrous filter" in which ㎛ sized fibers exist. These filters are porous having porosities from 70 to greater than 99%"

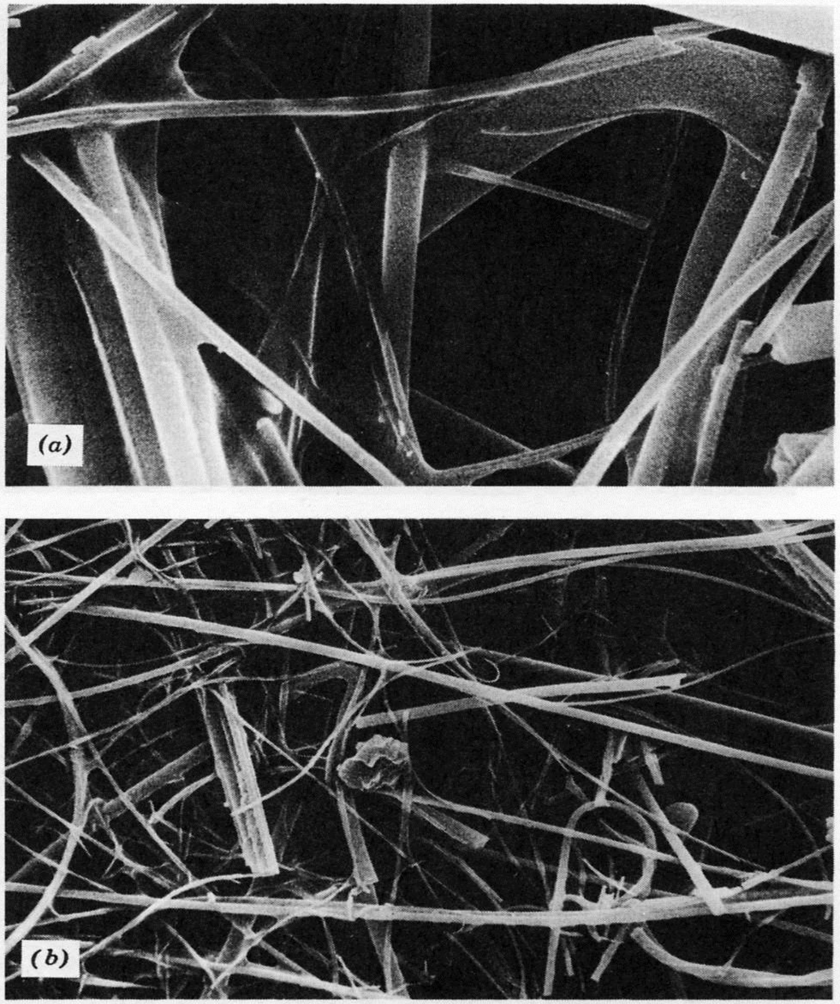

FIGURE 9.1 Scanning electron microscope photograph of a high-efficiency glass fiber filter. Magnification of (*a*) 4150× and (*b*) 800×.

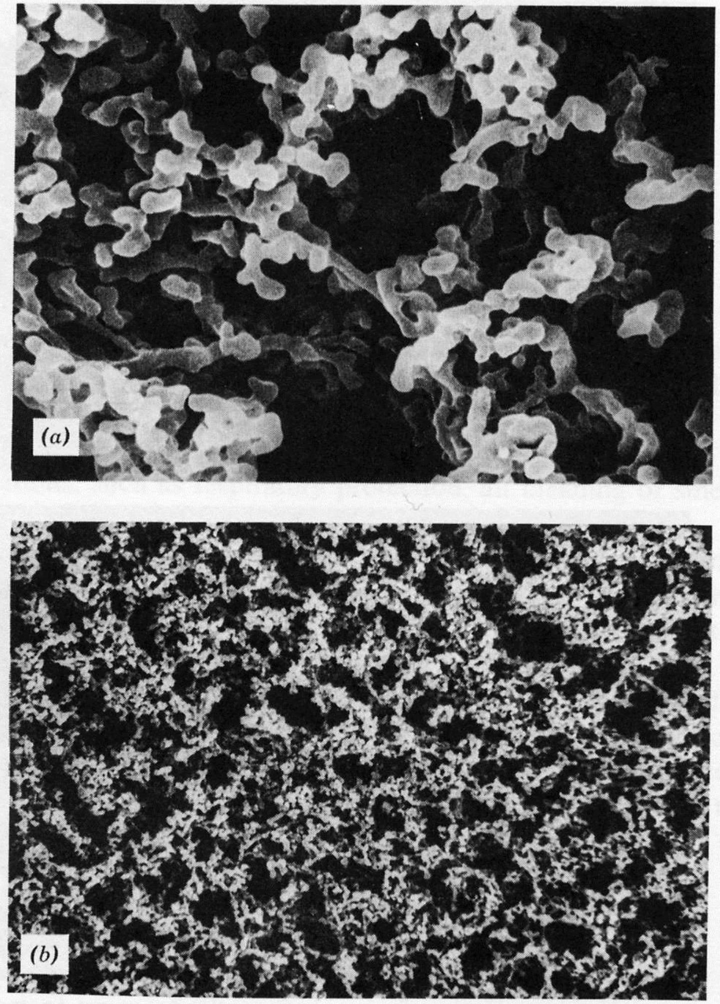

FIGURE 9.2 Scanning electron microscope photograph of a cellulose ester porous membrane filter with a pore size of 0.8 μm. Magnification of (*a*) 4150× and (*b*) 800×.

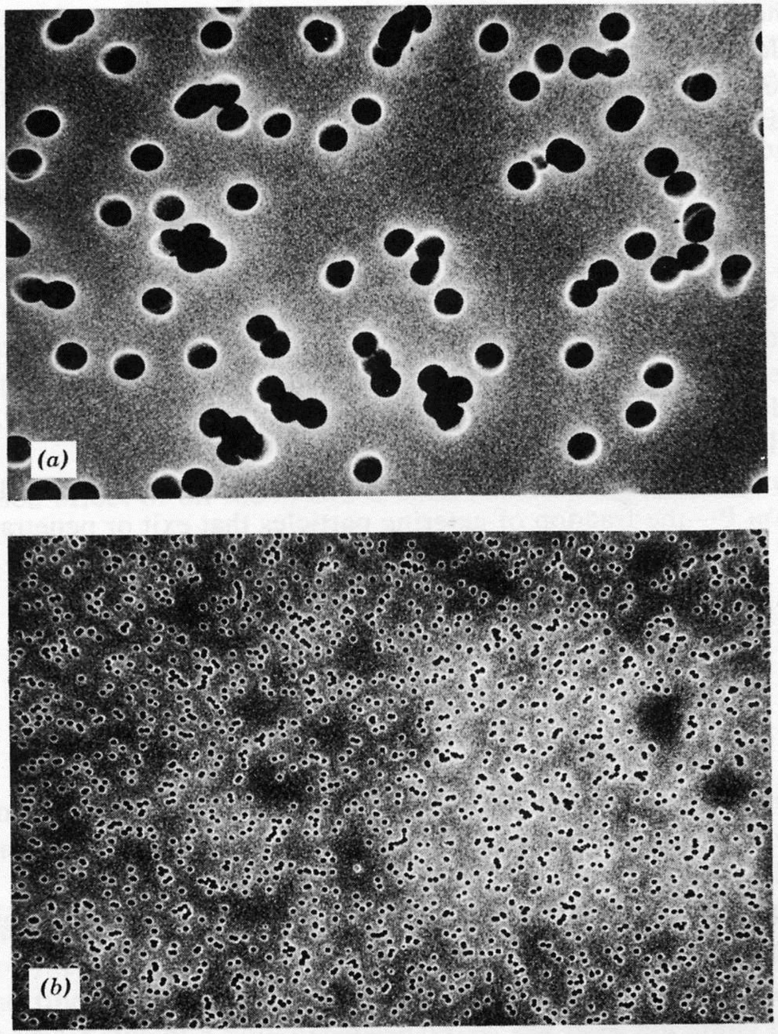

IGURE 9.3 Scanning electron microscope photograph of a capillary pore membrane filter ith a pore size of 0.8 μm. Magnification of (*a*) 4150× and (*b*) 800×.

“A common misconception is that aerosol filters could capture only particles larger than the open space. That is not the case. The aerosol filters do not behave like “sieves”. Since the adhesion force for ㎛ sized particle is large, the particles that contact “surface” by collision should be removed.

: The aerosol flow follows an irregular path through complex pore structure.

- porous membrane filter
- capillary pore membrane filter: has an array of microscopic cylindrical holes.
- Fabric filtration
- granular-bed filtration

→ In all of these filters, particles are captured by these different mechanism

① particle diffusion ② interception ③ impaction

ppt files

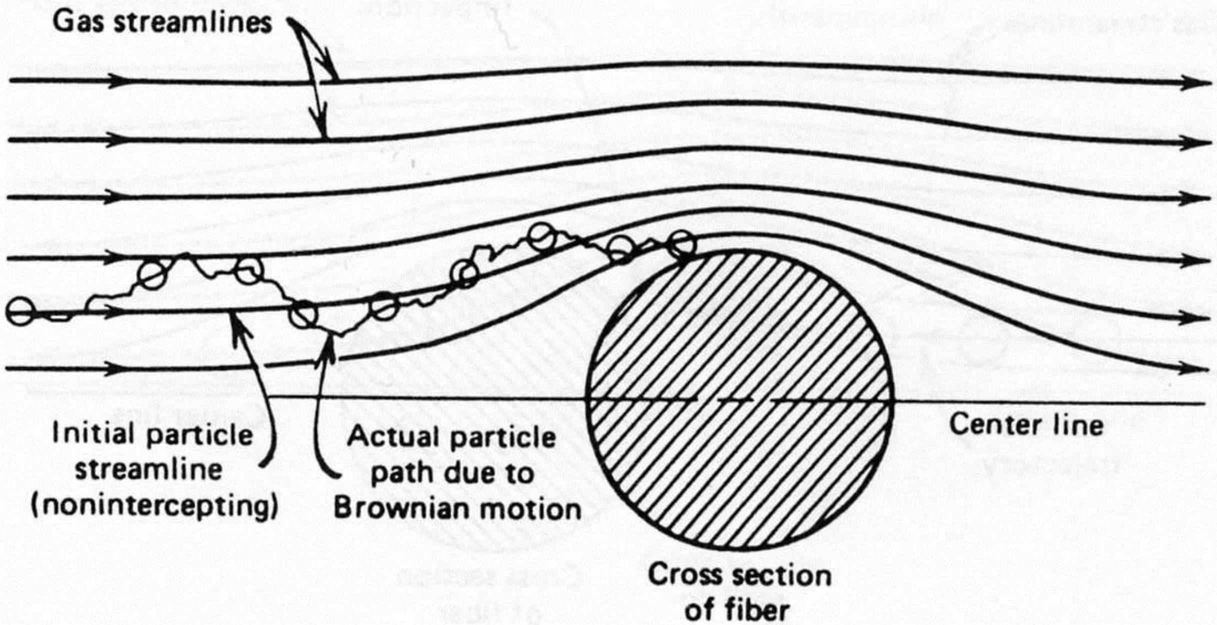

FIGURE 9.7 Single-fiber collection by diffusion.

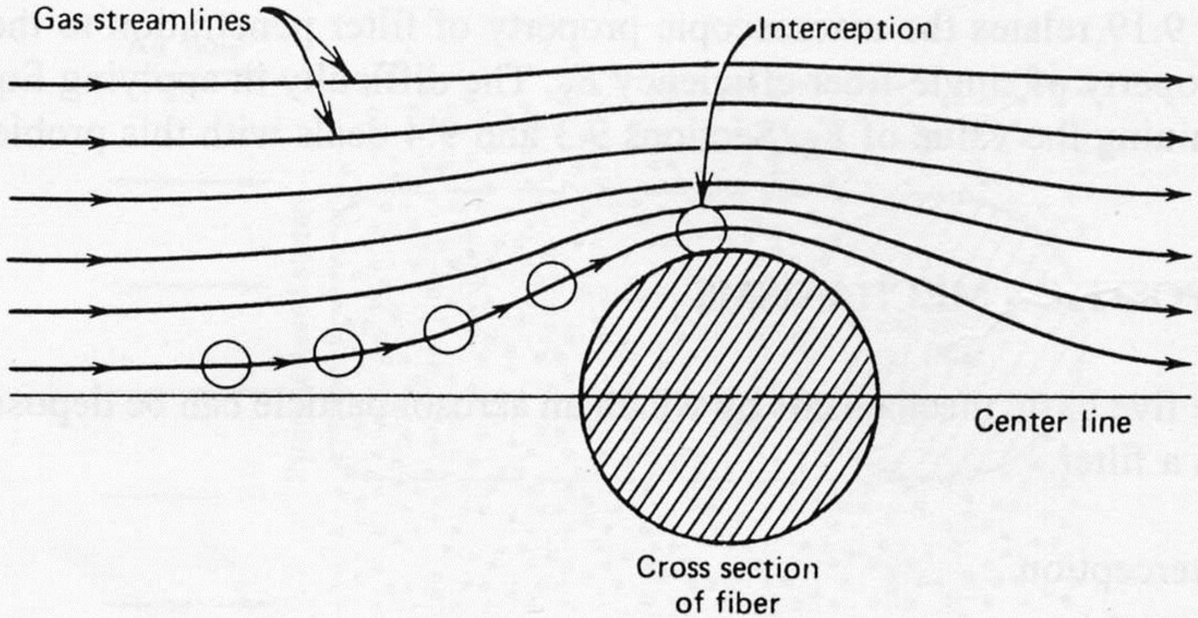

FIGURE 9.5 Single-fiber collection by interception.

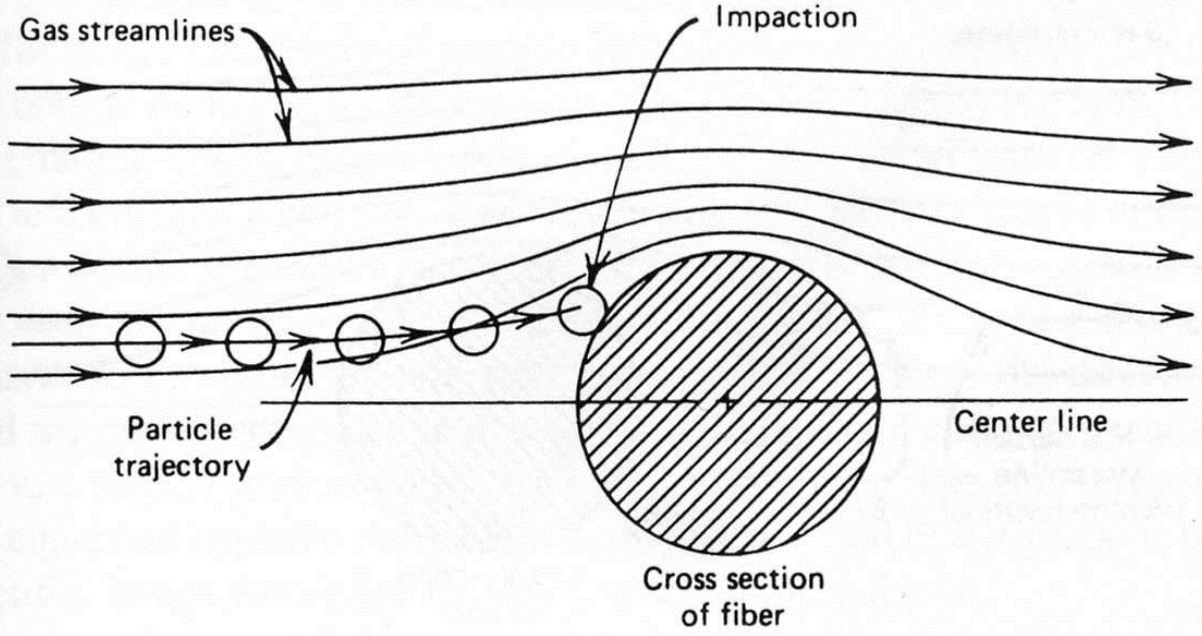

FIGURE 9.6 Single-fiber collection by impaction.

- Diffusional Deposition

Equation for convective diffusion

$$-D\frac{\partial n}{\partial x} \qquad\longrightarrow\qquad -D\frac{\partial n}{\partial x}-\frac{\partial}{\partial x}(D\frac{\partial n}{\partial x})dx$$

$$nv_x \qquad\longrightarrow\qquad nv_x+\frac{\partial}{\partial x}(nv_x)dx$$

$$nc_x \qquad\longrightarrow\qquad nc_x+\frac{\partial}{\partial x}(nc_x)dx$$

$\vec{c}$: drift velocity due to the external force

$$\vec{c}=\frac{\vec{F}}{f} \qquad \frac{\partial n}{\partial t}+\vec{v}\cdot\nabla n=D\nabla^2 n-\nabla\cdot\vec{c}n$$

$$\nabla\cdot\vec{v}=0$$

B.C. on solid surface?

Adhesion of particles

Aerosol particles attach firmly to any surface they contact due to adhesive force such as

- van der Waals force
- electrostatic force
- surface tension of adsorbed liquid films

van der Waals force is basically attractive force and acts over short distance away from a surface.

van der Waals forces result because electrically neutral particles develop instantaneous dipoles caused by fluctuations in the electron clouds surrounding the nucleus. These instantaneous dipoles induce dipoles on the surface. This causes “the attraction”. This force is dominant when particle is very near the surface within one radius of particles. So, particles adhere the surface.

That means there is no particle in gas very near the surface

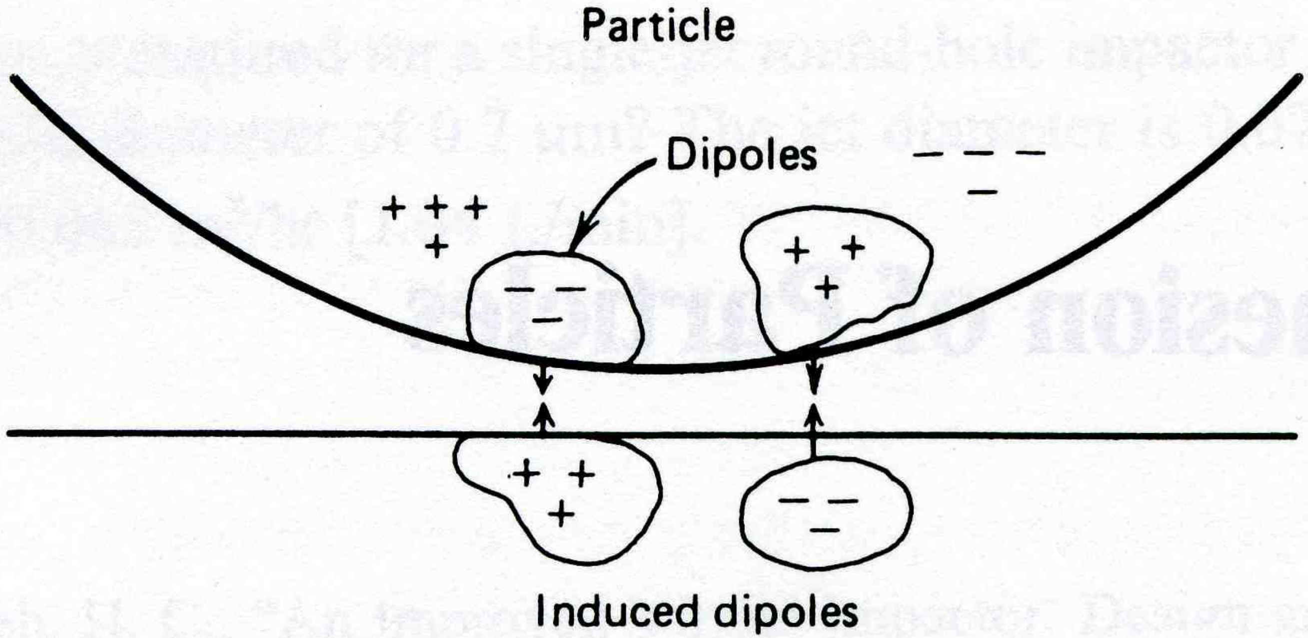

FIGURE 6.1 Van der Waals adhesive force.

$\longrightarrow$ n=0 at $x = d_p$

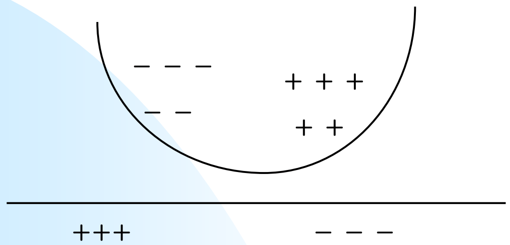

$$F_{adh} \propto \frac{d_p}{x^2}$$

After initial particle contact, the van der Waals and electrostatic forces gradually deform the asperities to reduce the separation distance and increase the contact area until the attractive forces balance the forces resisting deformation. The hardness of the materials involved controls the size of ultimate area of contact and therefore, the strength of the adhesive force. Flatterning can increase the adhesive force by up to fifteen fold in soft metals and more than a hundred-fold in plastics.

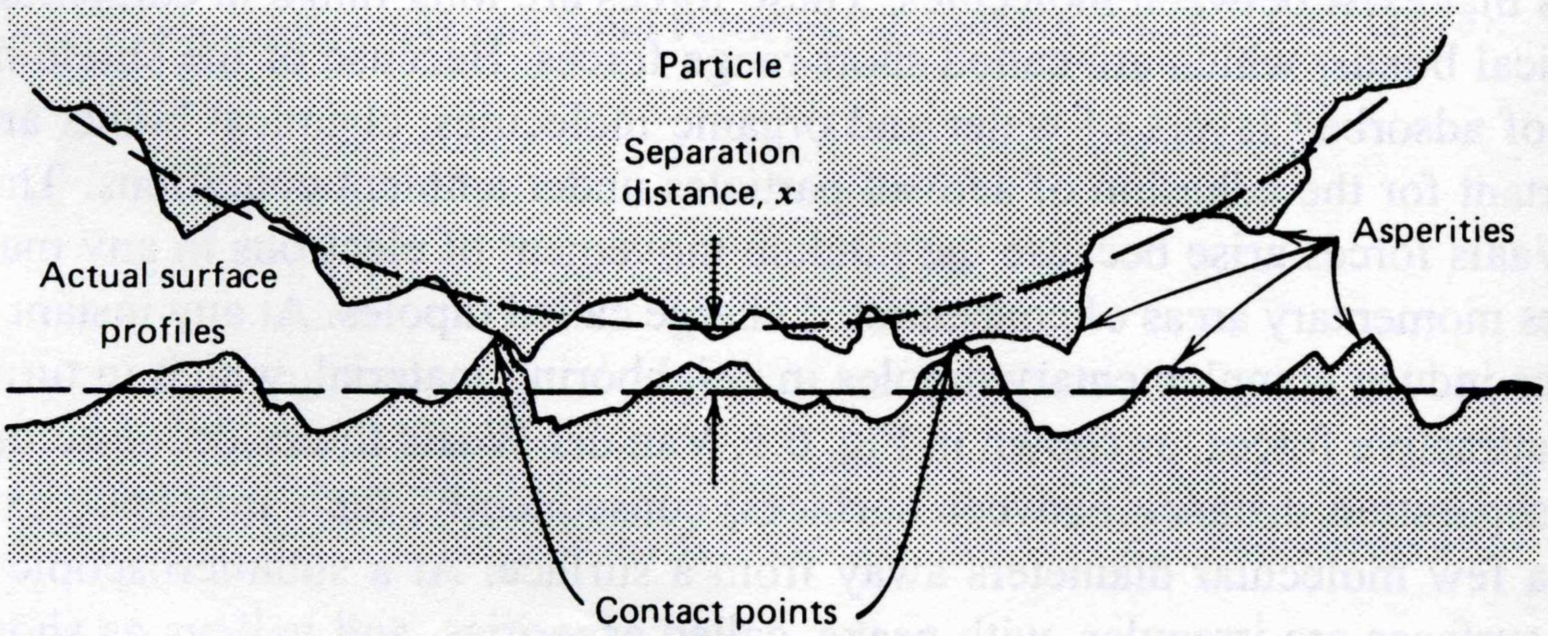

FIGURE 6.2 Submicroscopic surface contact geometry.

TABLE 6.1 Comparison of Adhesive, Gravitational, and Air Current Forces on Spherical Particles of Standard Density

Diameter (μm)	Force (N) Adhesion[a]	Gravity	Air Current (at 10 m/s [1000 cm/s])
0.1	10^{-8}	5×10^{-18}	2×10^{-10}
1.0	10^{-7}	5×10^{-15}	2×10^{-9}
10	10^{-6}	5×10^{-12}	3×10^{-8}
100	10^{-5}	5×10^{-9}	6×10^{-7}

[a]Calculated by Eq. 6.4 for 50% RH.

• <u>Detachment of particle</u>

Force is needed to overcome adhesive force, for example, centrifugal force or shear force due to velocity gradient.

“Adhesive forces are proportional to **d** while removal forces are proportional **d**^{3} for gravitational, vibrational, centrifugal and **d**^{2} for shear force.

This means that as the particle size become smaller, it becomes more difficult to remove particles from surface. The detachment of particle is an important topic for semi-conductor industry. Si Wafer contamination and cleaning problem.

- Particle Resuspension

Resuspension of particles is the result of detachment of particles usually by air jet. The larger the particle and the greater the air velocity, the greater the probability of resuspension.

- Particle bounce

If aerosol particle have low velocities, the particles lose the kinetic energy by deforming itself and the surface when they bombard the surface. However, at high velocity, part of its kinetic energy is dissipated in the deformation process and part is converted elastically to the kinetic energy for rebound. If the rebound energy exceeds the adhesive energy, then the particle will bounce away from the surface.

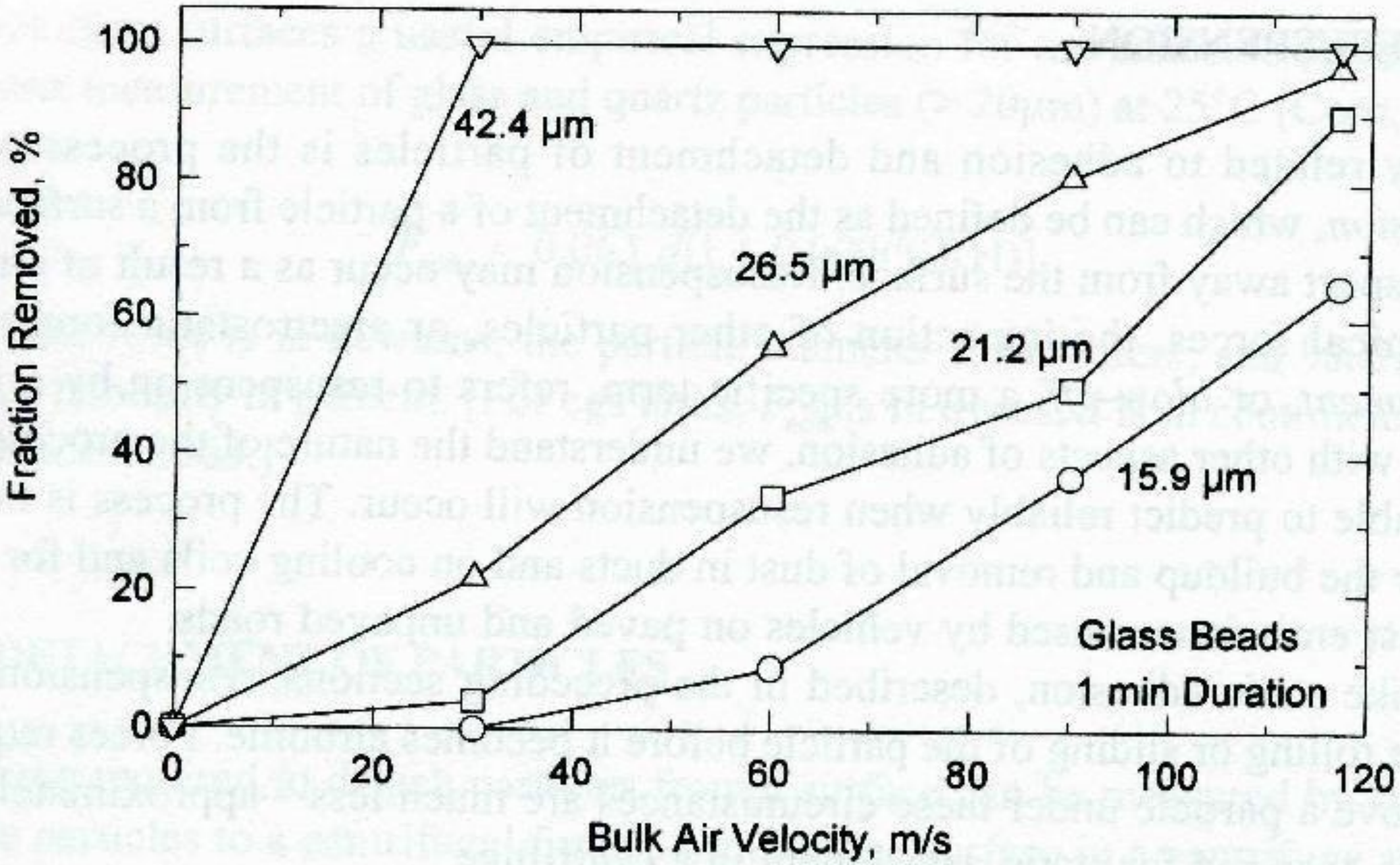

FIGURE 6.4 Particle reentrainment versus bulk air velocity for four particle sizes. Data from Corn and Stein (1965).

The harder the material, the larger the particle, the greater its velocity, the more likely bounce is to occur although surface roughness and hardness play also an important role. Coating surfaces with oil or grease tend to prevent the bouncing.

The kinetic energy required for bounce is given by Dahneke (1971) as

$$KE_b = \frac{d_p A(1-e^2)}{2xe^2}$$

Where x is separation distance (for smooth surface x< 1 ㎛

A: Hamaker constant

e: coefficient of restitution 0.73 < e < 0.81

Let us consider particle diffusion without external force.

Steady state

$$\vec{v}_1 \cdot \nabla_1 n_1 = \frac{1}{Pe} \nabla_1^2 n_1 \quad \longleftarrow \quad \text{dimensionless diffusion eq.}$$

$$\vec{v}_1 = \vec{v} / U \qquad \nabla_1 = L\nabla \qquad Pe = LU / D$$

Peclet number

$n = 0$ at $a_p / L = R$: interception parameter

(particles within a distance a_p of the surface would be intercepted even if diffusional effects were absent)

$n_1 = f$ (coordinate, Re, P_e, R)

$$J = -D \left.\frac{\partial n}{\partial y}\right)_{y=a_p} = -\frac{Dn_\infty}{L} \left.\frac{\partial n_1}{\partial y_1}\right)_{y_1=R}$$

$$\frac{JL}{n_\infty D} = f(\mathrm{Re}, Pe, R)$$

Sherwood number

total deposition per unit time

$$= JA = \frac{J}{n_\infty} \cdot n_\infty A$$

$$= \underline{k}A(n_\infty - 0)$$

like mass transfer coefficient or heat transfer coefficient

If R → 0 (point particle)

, interception can be negligible.

particle diffusion can be equally treated by gas diffusion

Diffusion to cylinders at low Reynolds number

(filter theory)

ppt files

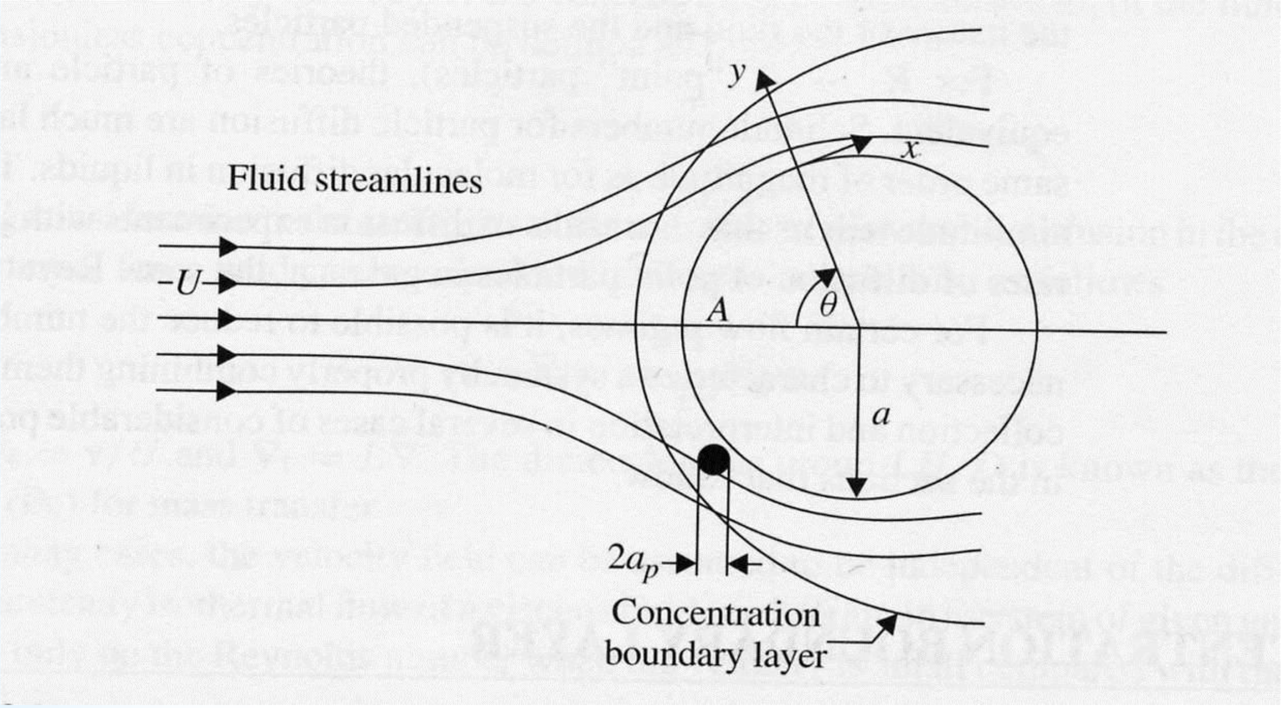
Fluid streamlines
y
x
−U
A
θ
a
2a_p
Concentration
boundary layer

* Diffusion to Cylinder : glass fibers filters

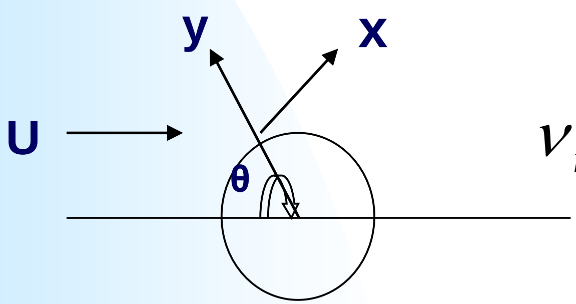

$$v_r \frac{\partial n}{\partial r} + v_\theta \frac{1}{r}\frac{\partial n}{\partial \theta} = D\left(\frac{\partial^2 n}{\partial r^2} + \frac{1}{r}\frac{\partial n}{\partial r} + \frac{1}{r^2}\frac{\partial^2 n}{\partial \theta^2}\right)$$

v_θ , v_r **should be known from NS equation.**

For small Re, near cylinder

$$\psi = AUa\sin\theta\left[\frac{r}{a}(2\ln\frac{r}{a}-1)+\frac{a}{r}\right]$$

$$P_e = \frac{Ud}{D} = Sc\cdot\mathrm{Re} \qquad (Sc = \frac{\nu}{D})$$

usually large number since D is small

boundary layer approximation angular diffusion can be negligible

$$\chi = a\theta$$

$$y = r - a$$

$$\therefore v_\theta \frac{\partial n}{\partial y} + v_r \frac{\partial n}{\partial y} = D \frac{\partial^2 n}{\partial y^2}$$

$$\begin{bmatrix} y = 0, n = 0 \\ y \to \infty, n \to n_\infty \end{bmatrix}$$

$$\left[\begin{array}{l} n=0 \quad at\ y=0 \\ n=n_\infty \quad at\ y=\infty \quad \text{(point particle)}\ (\ y=a_\phi) \end{array}\right.$$

$$v_\theta=+\frac{\partial\phi}{\partial y} \qquad v_r=-\frac{\partial\phi}{\partial x}$$

$$n(x,\ y) \ \rightarrow \ n(x,\ \phi)$$

$$\left.\frac{\partial}{\partial x}\right)_y=\left.\frac{\partial}{\partial x}\right)_\phi\left.\frac{\partial x}{\partial x}\right)_y+\left.\frac{\partial}{\partial \phi}\right)_x\left.\frac{\partial \phi}{\partial x}\right)_y=\left.\frac{\partial}{\partial x}\right)_\phi-v_r\left.\frac{\partial}{\partial \phi}\right)_x$$

$$\left.\frac{\partial}{\partial y}\right)_x=\left.\frac{\partial}{\partial x}\right)_\phi\left.\frac{\partial x}{\partial y}\right)_x+\left.\frac{\partial}{\partial \phi}\right)_x\left.\frac{\partial \phi}{\partial y}\right)_x=v_\theta\left.\frac{\partial}{\partial \phi}\right)_x$$

$$\therefore\ v_\theta\left(\frac{\partial n}{\partial x}-v_r\frac{\partial n}{\partial \phi}\right)+v_r v_\theta\frac{\partial n}{\partial \phi}=D\ v_\theta\frac{\partial}{\partial\phi}\left(v_\theta\frac{\partial n}{\partial\phi}\right)$$

$$\therefore\ \underline{\left.\frac{\partial n}{\partial x}\right)_\phi=D\ \frac{\partial}{\partial\phi}\left(v_\theta\frac{\partial n}{\partial\phi}\right)_x \ \rightarrow\ Eq.(3.15)}\ \text{Friedlander}$$

$$\phi=AUa\ \sin\frac{x}{a}\left(\left(\frac{y}{a}+1\right)\left(2\ln\left(\frac{y}{a}+1\right)-1\right)+\frac{1}{\frac{y}{a}+1}\right)$$

$$\frac{y}{a}\rightarrow 0 \qquad \frac{y}{a}=y_1 \qquad \frac{x}{a}=x_1$$

$$\phi\rightarrow 2AUa\ y_1^2\ \ \sin x_1 \quad \left(\phi\left(\frac{y}{a}\right)=\phi(0)+\phi'(0)\frac{y}{a}+\frac{\phi''(0)}{2\,!}\left(\frac{y}{a}\right)^2+\ldots\right)$$

$$v_\theta=\frac{\partial\phi}{\partial y}=\frac{1}{a}\frac{\partial\phi}{\partial y_1}=2AU\cdot 2y_1\sin x_1$$

$$y_1=\sqrt{\frac{\phi}{2AUa\sin x_1}} \qquad \therefore\ v_\theta=4AU\sin x_1\sqrt{\frac{\phi}{2AUa\sin x_1}}=\sqrt{\frac{8AU}{a}}\ \sin^{\frac{1}{2}} x_1\ \phi^{\frac{1}{2}}$$

$$\left.\frac{\partial n}{a\partial x_1}\right)_\phi=D\frac{\partial}{\partial\phi}\left(\sqrt{\frac{8AU}{a}}\ \sin^{\frac{1}{2}} x_1\,\phi^{\frac{1}{2}}\frac{\partial n}{\partial\phi}\right)$$

$$\frac{1}{\sqrt{8AUa}}\ \frac{1}{\sin^{\frac{1}{2}} x_1}\ \frac{\partial n}{\partial x_1}=D\frac{\partial}{\partial\phi}\left(\phi^{\frac{1}{2}}\frac{\partial n}{\partial\phi}\right)$$

$$V=\frac{1}{4}\int_0^{x_1} D\sqrt{8AUa}\ \sin^{\frac{1}{2}} x_1 dx_1 \qquad (x_1\rightarrow V)$$

$$Z=\sqrt{\phi},\quad Z^2=\phi,\quad 2ZdZ=d\phi \qquad (\phi\rightarrow Z)$$

$$\frac{1}{4}\ \frac{\partial n}{\partial V}=\frac{1}{4}\ \frac{1}{Z}\ \frac{\partial^2 n}{\partial Z^2} \qquad \therefore\ \frac{\partial n}{\partial V}=\frac{1}{Z}\ \frac{\partial^2 n}{\partial Z^2} \qquad \left(\begin{array}{lll} x=0=x_1 & & V=0 \\ y=0 & \phi=0 & Z=0 \\ y\rightarrow\infty & \phi\rightarrow\infty & Z\rightarrow\infty \end{array}\right)$$

Similarity Variable $\quad S=\dfrac{Z}{(9V)^{\frac{1}{3}}}$

$$n''(s)+3s^2n'(s)=0 \qquad \begin{array}{l} s\rightarrow 0\ \ (y\rightarrow 0\ \ z\rightarrow 0)\ \ n=0 \\ s\rightarrow\infty\ \ (x=0\ \ y\rightarrow\infty)\ \ n=n_\infty \end{array}$$

$$\therefore\ n=c_1\int_0^s e^{-s^3}ds+c_2$$

$$\therefore \quad \frac{n}{n_\infty} = \frac{\int_0^{s} e^{-s^3}\,ds}{\int_0^{\infty} e^{-s^3}\,ds} = \frac{\int_0^{\frac{Z}{(9V)^{\frac{1}{3}}}} e^{-s^3}\,ds}{0.893} \quad \left(\int_0^{\infty} e^{-s^3}\,ds = \Gamma\left(1\frac{1}{3}\right)\right)$$

$$J(x) = -D\frac{\partial n}{\partial y}\Big)_{y=0} = -D\frac{\partial n}{a\partial y_1}\Big)_{y_1=0}$$

$$\frac{\partial n}{\partial y_1}\Big)_{y_1=0} = a w_\theta \frac{\partial n}{\partial \phi}\Big)_{x_1}$$

$$= a\sqrt{\frac{8AU}{a}}\,\sin^{\frac{1}{2}} x_1 \phi^{\frac{1}{2}} \times \frac{\partial n}{\partial \phi}\Big)_{x_1} \quad \leftarrow \quad \frac{\partial n}{\partial \phi}\Big)_{x_1} = \frac{\partial n}{\partial Z}\frac{\partial Z}{\partial \phi} = \frac{1}{2\sqrt{\phi}}\frac{\partial n}{\partial Z}$$

$$= \frac{1}{2}\sqrt{8AUa}\,\sin^{\frac{1}{2}} x_1 \frac{\partial n}{\partial Z}\Big)_{Z=0}$$

$$= n_\infty\sqrt{2AUa}\,\sin^{\frac{1}{2}} x_1 \frac{1}{0.893}\frac{1}{(9V)^{\frac{1}{3}}}$$

$$\frac{\partial n}{\partial y_1}\Big)_{y_1=0} = n_\infty\sqrt{2AUa}\,\sin^{\frac{1}{2}} x_1 \frac{1}{0.893\times 9^{\frac{1}{3}}}\left[\frac{1}{4}\int_0^{x_1} D\sqrt{8AUa}\,\sin^{\frac{1}{2}} x_1\,dx_1\right]^{-\frac{1}{3}}$$

$$= n_\infty\sqrt{2AUa}\frac{1}{0.893\times 9^{\frac{1}{3}}}\left(\frac{D\sqrt{2AUa}}{2}\right)^{-\frac{1}{3}}\sin^{\frac{1}{2}} x_1\left[\int_0^{x_1}\sin^{\frac{1}{2}} x_1\,dx_1\right]^{-\frac{1}{3}}$$

$$= \frac{n_\infty}{0.893\times 9^{\frac{1}{3}}}\,2^{\frac{2}{3}}(AUa)^{\frac{1}{2}}\frac{1}{D^{\frac{1}{3}}(AUa)^{\frac{1}{6}}}\sin^{\frac{1}{2}} x_1\left[\int_0^{x_1}\sin^{\frac{1}{2}} x_1\,dx_1\right]^{-\frac{1}{3}}$$

total deposition

$$= 2D\int_0^{\pi}\left(\frac{\partial n}{\partial y_1}\right)_{y_1=0} dx_1 = k_{av}\pi d n_{\infty}$$ average mass transfer coefficient

$$\frac{k_{av}d}{D} = \frac{2}{\pi n_{\infty}}\int_0^{\pi}\frac{\partial n}{\partial y_1}\Big)_{y_1=0} dx_1$$

$$\left.\frac{\partial n}{\partial y_1}\right|_{y_1=0} = \frac{n_{\infty}}{0.893\times 9^{\frac{1}{3}}}\frac{2^{\frac{2}{3}}}{2^{\frac{1}{3}}}\left(\frac{U\cdot 2a}{D}\right)^{\frac{1}{3}} A^{\frac{1}{3}}\frac{\sin^{\frac{1}{2}}x_1}{\left[\int_0^{x_1}\sin^{\frac{1}{2}}x_1 dx_1\right]^{\frac{1}{3}}}$$

P

$$\frac{(AP_e)^{\frac{1}{3}}}{1.47} n_{\infty}\frac{\sin^{\frac{1}{2}}x_1}{\chi^{\frac{1}{3}}}$$ .....eq(3.24) in smoke.

$$\chi = \int_0^{x_1}\sin^{\frac{1}{2}}x_1 dx_1$$

$$\frac{k_{av}d}{D} = 1.17\,(AP_e)^{\frac{1}{3}}$$

↘ Sherwood no. (or mass transfer Nusselt number)

$$\frac{n_\infty}{\delta_c} \sim \frac{\partial n}{\partial y} \sim (AP_e)^{\frac{1}{3}} \frac{1}{a} \quad \therefore \frac{\delta_c}{a} \sim (AP_e)^{-\frac{1}{3}}$$ As $P_e \uparrow$ δ_c thinner

$$\eta_R = \frac{k_{av} \pi d n_\infty}{n_\infty U d} = 3.68 A^{\frac{1}{3}} P_e^{-\frac{2}{3}} \sim d^{-\frac{2}{3}}$$

η_R efficiency of removal

fine fibers are more efficient aerosol collector

$$\eta_R \sim D^{\frac{2}{3}} \sim d_p^{-\frac{2}{3}} \leftarrow f \sim d_p$$

$$\text{or} \quad d_p^{-\frac{4}{3}} \qquad f \sim d_p^2$$

∴ small particles are more efficiently removed by diffusion when $d_p < 0.5\mu m$.

- Effect of "interception"

for particles of finite diameters

ppt files for interception, impaction and deposition

$$u = 4AU\left(\frac{y}{a}\right)\sin\frac{x}{a}$$

$$v = -2AU\left(\frac{y}{a}\right)^2\cos\frac{x}{a}$$

$$n_1 = n/n_\infty \ , \quad y_1 = y/a_p \ , \quad x_1 = x/a$$

$$4y_1\sin x_1\frac{\partial n_1}{\partial x_1} - 2y_1^2\cos x_1\frac{\partial n_1}{\partial y_1} = \frac{Da^2}{AUa_p^3}\frac{\partial^2 n_1}{\partial y_1^2}$$

B.C. $\quad y_1 = 1 \qquad n = 0$

$$\therefore n_1 = f(x_1, y_1, R^3 PeA)$$

$$R = \frac{a_p}{a}$$: interception parameter

$$\eta_R n_\infty U d =$$ total deposition

η_R : efficiency of removal

$$= 2D \int_0^\pi a \left.\frac{\partial n}{\partial y}\right)_{y=a_p} dx_1$$

$$= 2D \frac{a}{a_p} n_\infty \int_0^\pi \left.\frac{\partial n_1}{\partial y_1}\right)_{y_1=1} dx_1$$

$$\therefore \eta_R RPe = f(RPe^{1/3} A^{1/3})$$

For point particle (R → 0), η_R should be independent of R

$$\therefore \eta_R R P_e = C R Pe^{1/3} A^{1/3}$$

$$\eta_R = C A^{1/3} Pe^{-\frac{2}{3}}$$

In the limiting case of $Pe \to \infty$ $(D \to 0)$

, there is no “diffusion”.

Particles follow the streamline and deposit when a streamline passes within one radius of particle.

This is called “direct interception”.

$$\eta_R R Pe = C R^3 Pe A \qquad \therefore \eta_{Re} = \underline{\underline{C A R^2}}$$

Or $$\eta_R = \frac{2n_\infty \int_0^{\pi/2} v_{y=a_p} dx}{U d n_\infty} = 2AR^2$$

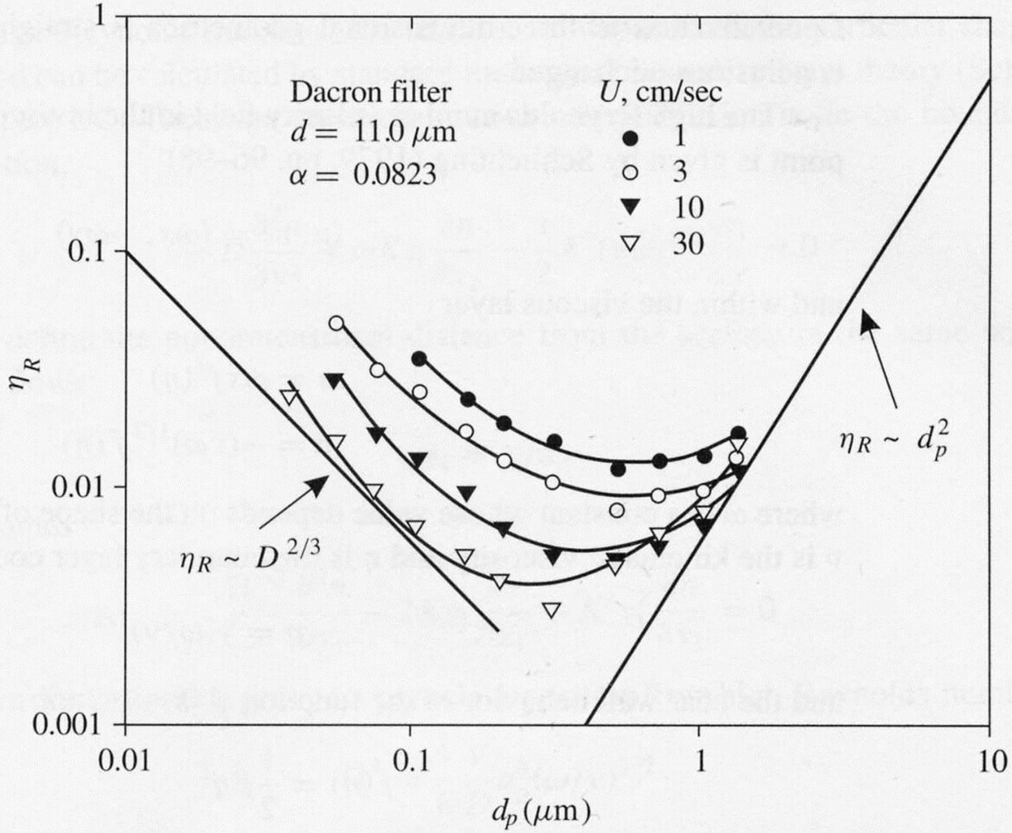

Figure 3.6 Efficiency minimum for single fiber removal efficiency for particles of finite diameter. For very small particles, diffusion controls according to (3.38) and $\eta_R \sim D^{2/3}$. The different curves result from the effects of velocity. In the interception range according to (3.39), $\eta_R \sim d_p^2$, and is practically independent of gas velocity (data of Lee and Liu, 1982a).

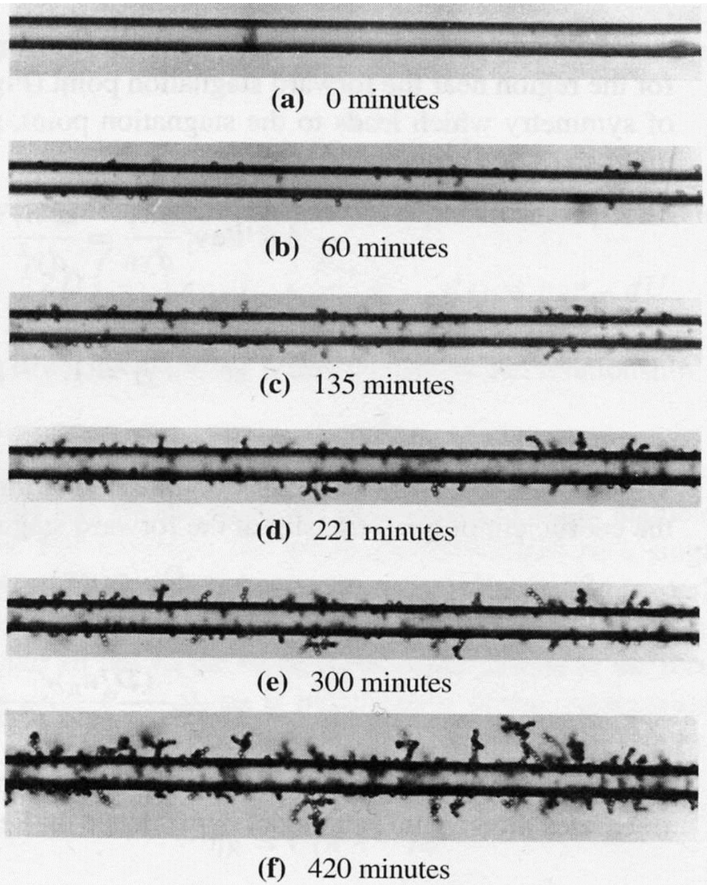

Figure 3.3 Deposits of 1.3-μm polystyrene latex particles on an 8.7-μm glass fiber mounted normal to an aerosol flow and exposed for increasing periods of time. The air velocity was 13.8 cm/sec, and the particle concentration was about 1000 cm^{-3}. Photos by C. E. Billings (1966). The principal mechanism of deposition was probably direct interception. Fractal-like structures develop as the particles deposit.

Filter

Experimental validation for single fiber collection efficiency is difficult.

Effective single-fiber removal efficiency can be determined by measuring the fraction of particles collected in a bed of fibers.

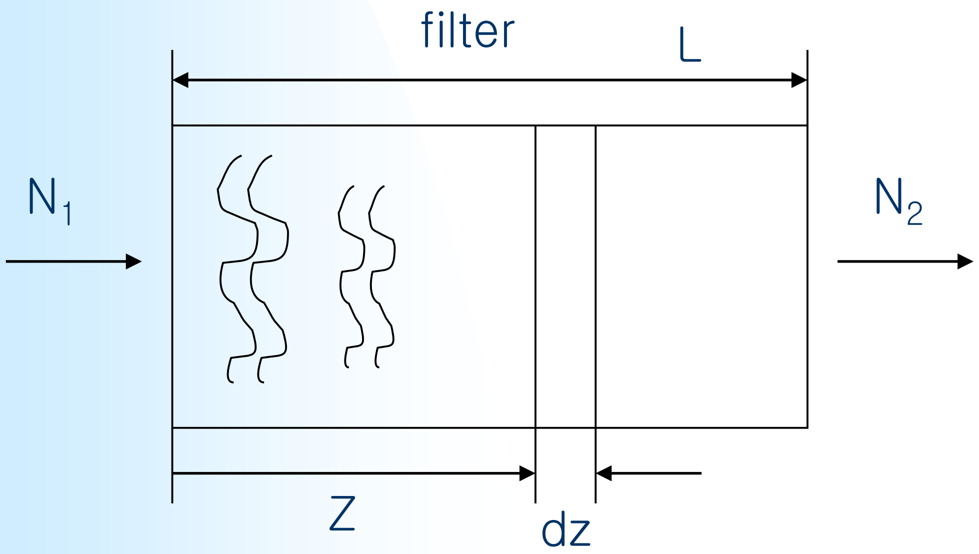

α: fraction of solid

$$\alpha = \frac{\frac{\pi}{4} d^2 L_f n_0}{A_c dz}$$

n_0 : number of fibers within dz

$$\eta_R U_\infty n_z dL_f n_0 = A_c \bar{u}(n_z - n_{z+dz})$$

$$U_\infty = \frac{\bar{u}}{1-\alpha}$$

U_∞ : approaching velocity

$$-\frac{dn}{dz} = \eta_R \frac{d}{1-\alpha} \frac{\alpha}{\frac{\pi}{4}d^2} n$$

$$L_f n_0 = \frac{\alpha A_c dz}{\frac{\pi}{4}d^2}$$

$$\ln\frac{N_1}{N_2} = \eta_R \frac{\alpha}{1-\alpha} \frac{L}{\frac{\pi}{4}d}$$

$$\eta_R = \frac{\pi d}{4\alpha L}(1-\alpha)\ln\frac{N_1}{N_2}$$

→ single fiber removal efficiency

Overall efficiency of filter

$$\eta_b = 1 - \frac{N_2}{N_1} = 1 - \exp\left[-\frac{4\alpha \eta_R L}{\pi(1-\alpha)d} \right]$$

ppt file

for comparison with experiment

- Diffusion in a Tube flow

$$S_c = \frac{\nu}{D} >> 1$$

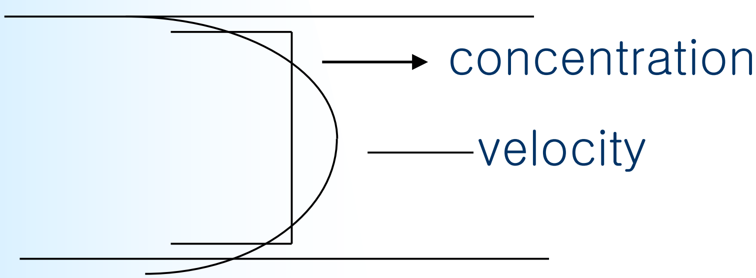

$$u\frac{\partial n}{\partial x} = D\frac{1}{r}\frac{\partial}{\partial r}(r\frac{\partial n}{\partial r})$$

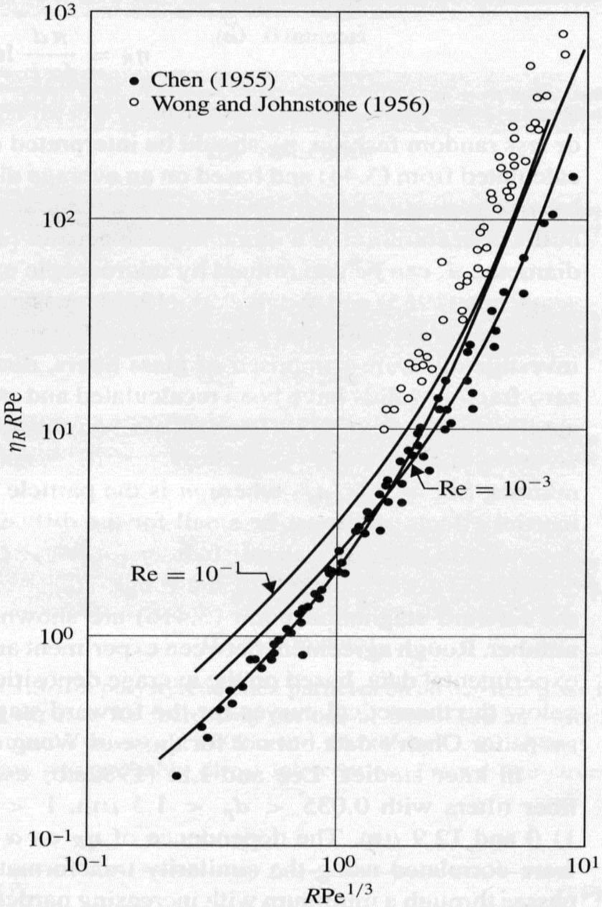

Figure 3.5 Comparison of experimentally observed deposition rates on glass fiber mats for dioctyphthalate (Chen, 1955) and sulfuric acid (Wong et al., 1956) aerosols with theory for the forward stagnation point of single cylinders (Friedlander, 1967). The theoretical curves for $Re = 10^{-1}$ and 10^{-3} were calculated from (3.41b). For all data points the Stokes number was less than 0.5. Agreement with the data of Chen is particularly good. Theory for the forward stagnation point should fall higher than the experimental transfer rates, which are averaged over the fiber surface. The heavy line is an approximate best fit with the correct limiting behavior. The figure supports the use of the similarity transformation (3.37). Similar results have been reported by Lee and Liu (1982a,b). The lower portion of the curve corresponds to the range in which diffusion is controlling and the upper portion corresponds to the direct interception range.

$$\begin{cases} r = a & n = 0 \\ r = 0 & \dfrac{\partial n}{\partial r} = 0 \\ x = 0 & n = n_0 \end{cases}$$

→ same as Graetz problem
(Thermally developing problem)

Diffusion in a Tube flow

$$\frac{n}{n_0} = \sum_{n=0}^{\infty} C_n R_n \left(\frac{r}{a}\right) \exp\left(-\lambda_n^2 \frac{x}{aPe}\right)$$

$$\frac{n_{av}}{n_0} = 8 \sum \frac{G_n}{\lambda_n^2} \exp(-\lambda_n^2 x_1) \qquad G_n = -\frac{C_n}{2} R_n^{'} \quad \textbf{(1)}$$

$$n_{av} = \frac{2}{a^2 U} \int_0^a unrdr$$

(Bulk average 혹은 Mixing Cup average)

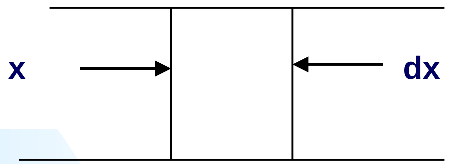

$$J = -D\frac{\partial n}{\partial r})_{r=a} = k_x n_{av}$$

$$\therefore k_x n_{av} \cdot 2\pi a dx = -dn_{av}\pi a^2 U$$

$$\therefore \frac{2}{aU}k_x dx = -\frac{dn_{av}}{n_{av}} \qquad \frac{2}{au}\int_0^x k_x d_x = \ln\frac{n_0}{n_{av}}$$

$$k_{av} = \frac{1}{x}\int_0^x k_x d_x$$

$$\therefore \frac{2k_{av}a}{D} = \frac{1}{2x_1}\ln\frac{n_0}{n_{av}}$$

$$x_1 = \frac{x}{a \cdot \frac{Ud}{D}} \propto \frac{4DL}{\pi d^2 U} = \frac{DL}{Q} = \mu$$

$$\frac{n_2}{n_1} = 1 - 2.56\Pi^{2/3} + 1.2\Pi + 0.1767\Pi^{4/3} + \cdots \quad \text{(3-74)}$$

$$\Pi = \pi\mu < 0.02$$

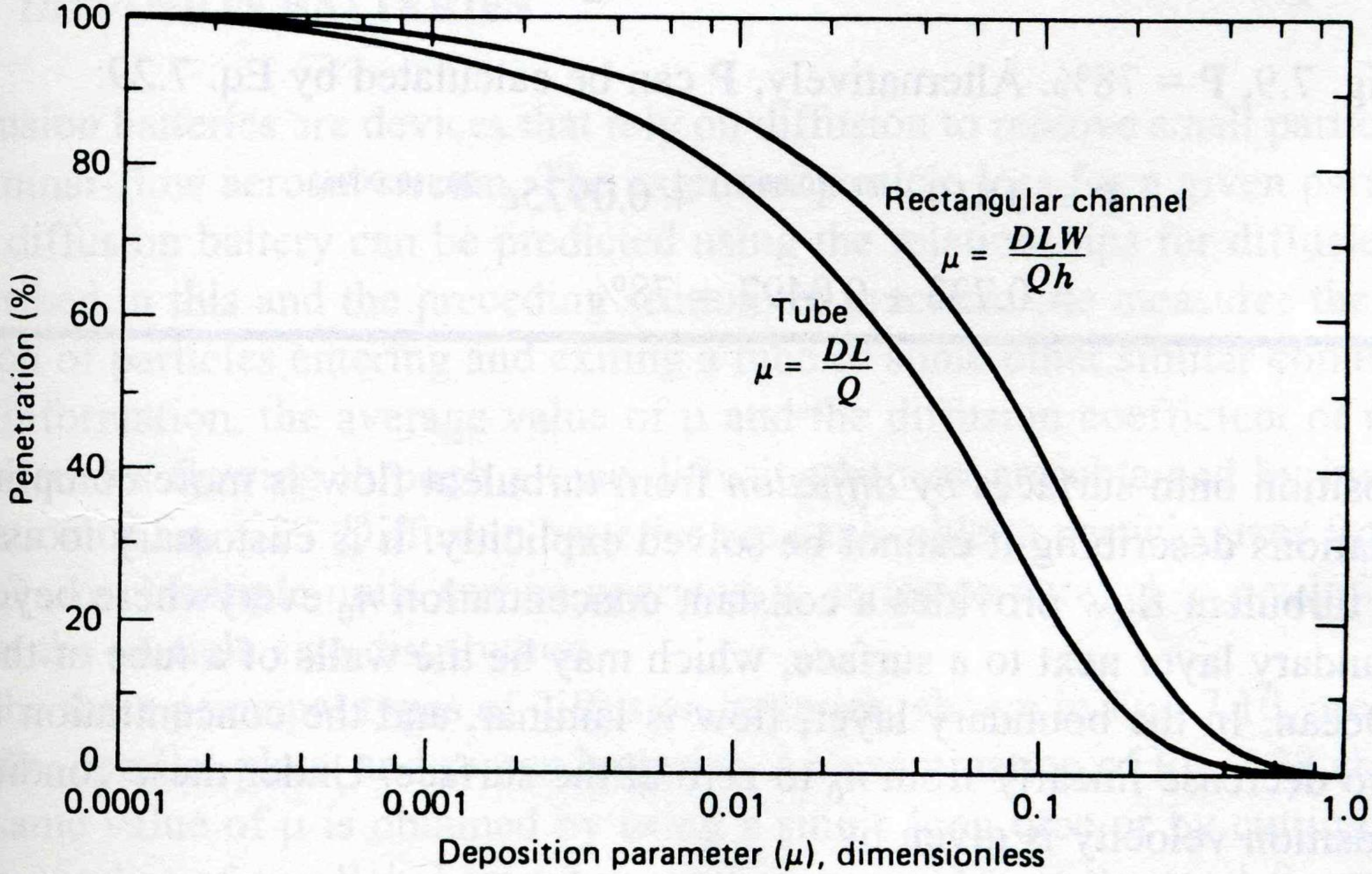

FIGURE 7.9 Penetration versus deposition parameter for circular tubes and for channels with a rectangular cross section.

Diffusion Battery

- monodisperse aerosol – can measure particle size

- polydisperse aerosol

  → average diffusion coefficient

  → diffusion equivalent diameter

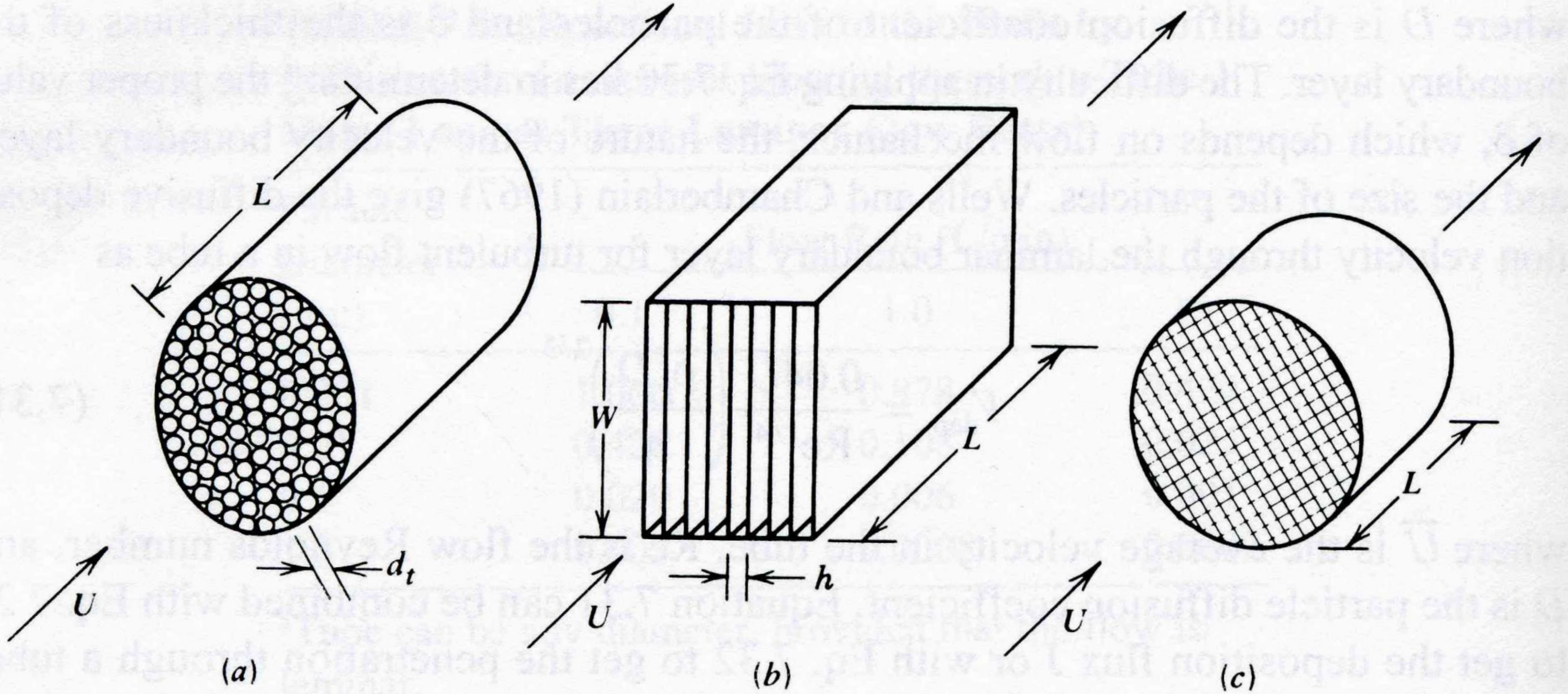

FIGURE 7.10 Three types of diffusion batteries. (*a*) Tube bundle. (*b*) Parallel plate, or rectangular channel. (*c*) Screen.

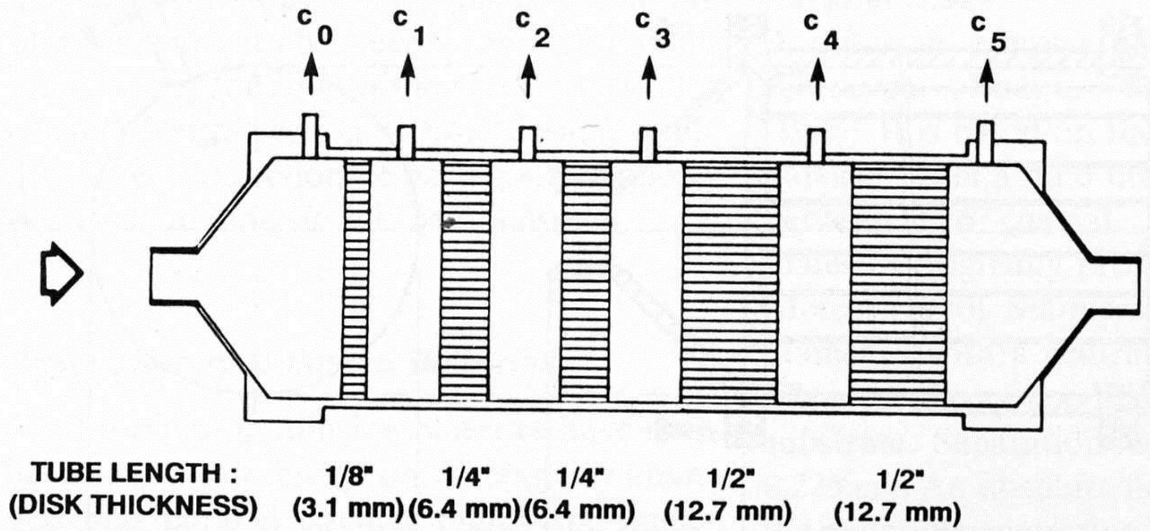

FIGURE 19-11. Schematic Diagram of a Five-Stage Diffusion Battery Consisting of a Stainless Steel Collimated Hole Structure.

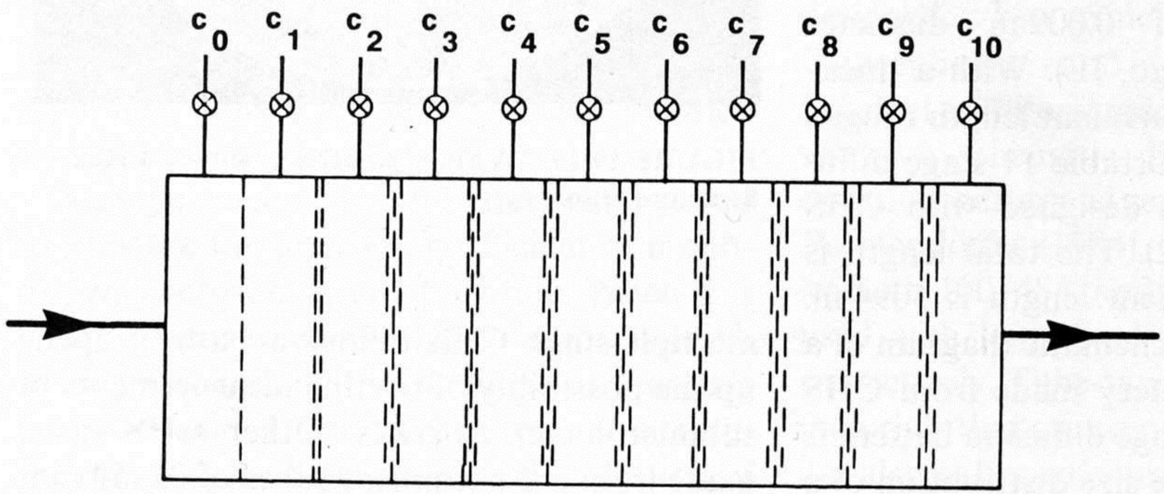

FIGURE 19-12. Schematic Diagram of a Ten-Stage Screen-Type Diffusion Battery.

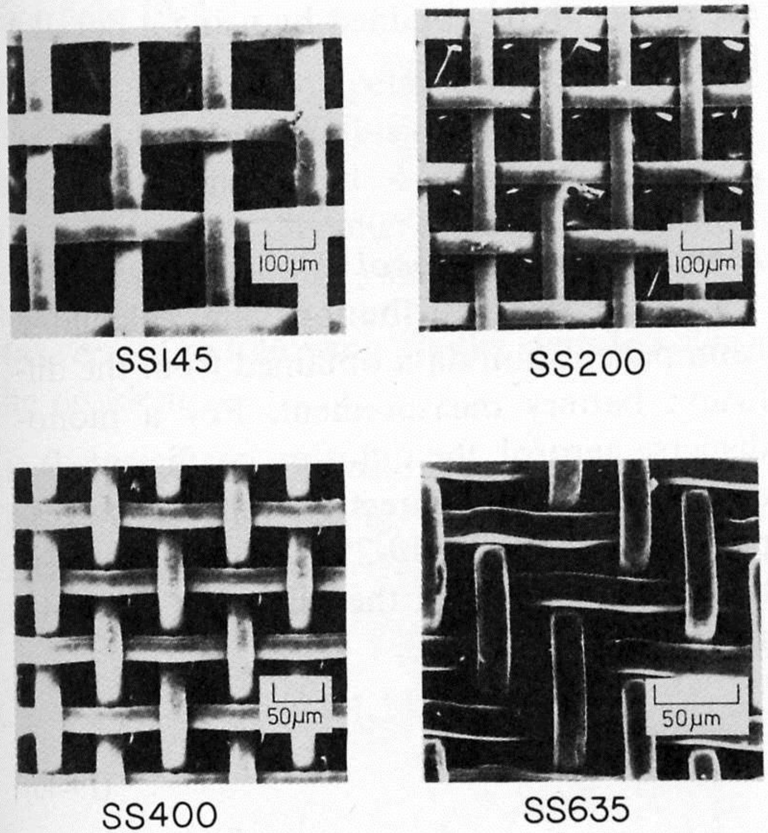

FIGURE 19-13. Photomicrograph of Stainless Mesh Screens.